Proc. Natl. Acad. Sci. USA
Vol. 80, pp. 5798–5802, September 1983
Physics

Viscous, resistive magnetohydrodynamic stability computed by spectral techniques

(transition to turbulence/"tearing modes"/dissipative magnetohydrodynamic instabilities)

R. B. DAHLBURG*, T. A. ZANG*, D. MONTGOMERY*, AND M. Y. HUSSAINI†

*College of William and Mary, Williamsburg, Virginia 23185; and †Institute for Computer Applications in Science and Engineering, National Aeronautics and Space Administration Langley Research Center, Hampton, Virginia 23665

Communicated by Peter D. Lax, June 2, 1983

ABSTRACT **Expansions in Chebyshev polynomials are used to study the linear stability of one-dimensional magnetohydrodynamic quasiequilibria, in the presence of finite resistivity and viscosity. The method is modeled on the one used by Orszag in accurate computation of solutions of the Orr–Sommerfeld equation. Two Reynolds-like numbers involving Alfvén speeds, length scales, kinematic viscosity, and magnetic diffusivity govern the stability boundaries, which are determined by the *geometric mean* of the two Reynolds-like numbers. Marginal stability curves, growth rates versus Reynolds-like numbers, and growth rates versus parallel wave numbers are exhibited. A numerical result that appears general is that instability has been found to be associated with inflection points in the current profile, though no general analytical proof has emerged. It is possible that nonlinear subcritical three-dimensional instabilities may exist, similar to those in Poiseuille and Couette flow.**

The linear stability of plane shear flows has been one of the most intensively studied hydrodynamic problems from the time of Rayleigh, since it was thought to hold clues to the nature of turbulence [see, e.g., Lin (1) or Maslowe (2)]. Although the linear theory alone appears to be inadequate to predict the onset of shear flow instabilities, it remains an important first step in any discussion of the problem. We report here on an analogous problem in incompressible magnetohydrodynamics (MHD). We report numerical solutions of the quiescent-MHD analogue of the Orr–Sommerfeld equation, using spectral methods developed by Orszag (3).

We begin with the incompressible MHD equations in a familiar dimensionless form:

$$\frac{\partial \mathbf{B}}{\partial t} = \nabla \times (\mathbf{v} \times \mathbf{B}) + \frac{1}{S}\nabla^2 \mathbf{B}, \qquad [1]$$

$$\frac{\partial \mathbf{v}}{\partial t} = -\mathbf{v}\cdot\nabla\mathbf{v} + \mathbf{B}\cdot\nabla\mathbf{B} - \nabla p + \frac{1}{M}\nabla^2 \mathbf{v}, \qquad [2]$$

supplemented by the conditions that $\nabla\cdot\mathbf{v} = 0$ and $\nabla\cdot\mathbf{B} = 0$. $\mathbf{B}$ is the magnetic field measured in units of a mean magnetic field magnitude $\overline{B}$, say. The velocity field is measured in units of the mean Alfvén speed $C_A \equiv \overline{B}(4\pi\rho)^{-1/2}$, where ρ is the mass density, assumed uniform. The dimensionless pressure is p, and it is determined by solving the Poisson equation that results from taking the divergence of Eq. 2 and using $\nabla\cdot\partial\mathbf{v}/\partial t = 0$. The dimensionless numbers S and M have the structure of Reynolds numbers. $S \equiv C_A L/\eta$ is the Lundquist number, where η is the magnetic diffusivity and L is a macroscopic length scale; $M \equiv C_A L/\nu$ is a viscous analogue, where ν is a kinematic viscosity. Both η and ν are assumed to be scalars. The regime of most interest is that in which S and M are both substantially greater than unity.

The boundary conditions are taken to be those appropriate to a perfectly conducting, mechanically impenetrable wall bounding a viscous, resistive magnetofluid: $\mathbf{v} = 0$, $\hat{n}\cdot\mathbf{B} = 0$, and $\hat{n}\times(\nabla\times\mathbf{B}) = 0$, where $\hat{n}$ is the unit normal at the wall.

We study the linear stability of the quasiequilibrium $\mathbf{B}^{(0)} = (B_0(y),0,0)$ and $\mathbf{v}^{(0)} = (0,0,0)$ between parallel, plane infinite boundaries at $y = 1$ and $y = -1$. The current density is in the z direction only: $j_0 = -DB_0$, where $D \equiv d/dy$. The configuration described is not a true equilibrium, and the magnetic field will resistively decay according to $B_0(y,t) = \exp(S^{-1}t\nabla^2)\cdot B_0(y,0)$. The temporal variation will be assumed to be slow enough to be negligible: $B_0(y,t) \cong B_0(y,0) = B_0(y)$. This implies that our stability boundaries will not be accurate in regions of small S; there is in this feature a conceptual difference from the already much-studied (4–6) problem of a mean flow parallel to a uniform magnetic field with no current, which is a true equilibrium, and from Hartmann flow (6).

A linear expansion $\mathbf{B} = \mathbf{B}^{(0)} + \mathbf{B}^{(1)}$, $\mathbf{v} = \mathbf{v}^{(1)}$, is assumed, with products of $\mathbf{v}^{(1)}$ and $\mathbf{B}^{(1)}$ being discarded everywhere in the equations of motion. Manipulating the components of the resulting linear equations, we may prove a Squire's theorem (1), which implies that for the location of the most unstable modes it suffices to consider the two-dimensional case: $\partial/\partial z$ may be set equal to zero throughout. All variations with the parallel coordinate x and the time t are assumed to be contained in a factor $\exp(i\alpha x - i\omega t)$, with α an arbitrary, real, parallel wave number and $\omega = \omega_r + i\omega_i$ a complex eigenvalue. Dahlburg and Montgomery (7) have given the eigenvalue equations in the form used here:

$$(D^2 - \alpha^2)^2 v = -i\omega M(D^2 - \alpha^2)v - i\alpha M B_0(D^2 - \alpha^2)b + i\alpha M(D^2 B_0)b \qquad [3]$$

and

$$(D^2 - \alpha^2 + i\omega S)b = -i\alpha S B_0 v. \qquad [4]$$

Here b and v are the y components of $\mathbf{B}^{(1)}$ and $\mathbf{v}^{(1)}$ and depend only upon y. The boundary conditions become $v = 0$, $Dv = 0$, and $b = 0$ at $y = 1$ and $y = -1$.

Eqs. 3 and 4 are the magnetostatic analogue of the Orr–Sommerfeld equation, which in the same notation (1–3) is $(D^2 - \alpha^2)^2 v = i\alpha R[(U_0 - \omega/\alpha)(D^2 - \alpha^2)v - (D^2 U_0)v]$, where $U_0(y)$ is a shear flow velocity profile in the x direction, R is the Reynolds number, and the boundary conditions are that $v = 0$, $Dv = 0$ at $y = \pm 1$.

The publication costs of this article were defrayed in part by page charge payment. This article must therefore be hereby marked "*advertisement*" in accordance with 18 U.S.C. §1734 solely to indicate this fact.

Abbreviation: MHD, magnetohydrodynamics.

Eqs. 3 and 4 are quite similar to eigenvalue problems arising in connection with confinement of thermonuclear plasmas. The literature on "tearing modes" is extensive, and we may cite the central papers of Furth *et al.* (8, 9), of Wesson (10), of Coppi *et al.* (11), and of Dibiase and Killeen (12). Concern has frequently been with the nonviscous ($M = \infty$) case, which lowers the order of the differential equations. Viscous results from a linear initial-value computation have been reported by Dibiase and Killeen (12) for the compressible case, and, to the extent that the results can be compared, ours do not appear to disagree with theirs. Because for plasmas of interest to date, the calculated viscosity coefficients give estimates of ν at as great as those for η [see, e.g., Braginskii (13)], it seems desirable to retain viscous effects even at the price of raising the order of the eigenvalue problem to the point where results can be extracted only numerically.

Analytical information is difficult to extract even for the simpler Orr–Sommerfeld equation [e.g., Maslowe (2) or Reid (14)] and numerical solution is indicated here. We use a spectral technique closely patterned on the method used by Orszag (3) to calculate critical Reynolds numbers for Poiseuille flow to six-figure accuracy. It is to be expected that spectral methods will find further applications in plasma physics beyond the immediate ones.

The mean magnetic field $B_0(y)$ and the perturbation quantities v and b are expanded in truncated Chebyshev series

$$B_0(y) = \sum_{n=0}^{N} \tilde{B}_n T_n(y)$$

$$v(y) = \sum_{n=0}^{N} \tilde{v}_n T_n(y) \qquad [5]$$

$$b(y) = \sum_{n=0}^{N} \tilde{b}_n T_n(y),$$

where $T_n(y)$ is the nth Chebyshev polynomial of the first kind, and $\tilde{B}_n$, $\tilde{v}_n$, and $\tilde{b}_n$ are the respective expansion coefficients.

The equations satisfied by the (unknown) expansion coefficients are obtained by substituting the $N \to \infty$ expansions of Eq. 5 into Eqs. 3 and 4, each of which produces a countably infinite number of equations in the expansion coefficients for $n = 0, 1, 2, \ldots$, when the orthogonality and recursion relations (3) are used. We then set all coefficients beyond $n = N$ to zero and use the $n = 0$ to $n = N - 4$ equations from Eq. 3, the $n = 0$ to $N - 2$ equations from Eq. 4, and the boundary conditions $\Sigma_{n=0}^{N} \tilde{v}_n = 0$, $\Sigma_{n=0}^{N} (-1)^n \tilde{v}_n = 0$, $\Sigma_{n=1}^{N} n^2 \tilde{v}_n = 0$, $\Sigma_{n=1}^{N} (-1)^n n^2 \tilde{v}_n = 0$, $\Sigma_{n=0}^{N} \tilde{b}_n = 0$, and $\Sigma_{n=0}^{N} (-1)^n \tilde{b}_n = 0$. This method of truncation is called the "tau approximation" after Lanczos (15); Gottlieb and Orszag (16) give a general discussion of the use of the tau method in the Chebyshev case.

This spectral discretization process yields a generalized eigenvalue problem that can be written as $Ax = \omega Bx$, where the vector $x = (\tilde{v}_0, \tilde{v}_1, \ldots \tilde{v}_N, \tilde{b}_0, \tilde{b}_1, \ldots \tilde{b}_N)$, and A and B are nonsymmetric $(2N + 2)$ by $(2N + 2)$ square matrices.

As is customary for this type of stability problem, either global or local methods are used to determine the eigenvalues. The global method is based on the QR algorithm [Wilkinson (17), Gary and Helgason (18)] and produces a full spectrum of eigenvalues. It is employed when no good guess for the least stable (or most unstable) eigenvalue is available. The local method employs inverse Rayleigh iteration (17) and converges to the eigenvalue (and its associated eigenfunction) closest to the initial guess for the eigenvalue. The global method may be used to identify the eigenvalue with the largest imaginary part, and the local method is useful when making a series of computations in which either the wavenumber or the Reynolds numbers are slowly varied.

For functions $B_0(y)$ that are antisymmetric about $y = 0$, it is readily inferred from Eqs. 3 and 4 that v and b are of opposite parity when reflected about $y = 0$. We have confined attention to the case $B_0(y) = -B_0(-y)$ with an associated current distribution $j_0 = -DB_0$, which has even parity about $y = 0$: the classic "sheet pinch" configuration. This configuration [indeed, any $B_0(y)$ profile] can be rigorously proved to be stable in the ideal limit ($M = \infty$, $S = \infty$); any instabilities must result from finite values of S or M or (in our case) both.

We have solved for the several eigenfunctions corresponding to the largest values of ω_i for four different antisymmetric profiles $B_0(y)$:

$$\begin{aligned} B_0^{\mathrm{I}}(y) &\equiv y - y^3/3 \\ B_0^{\mathrm{II}}(y) &\equiv \tan^{-1}\gamma y - \gamma y(\gamma^2 + 1)^{-1} \\ B_0^{\mathrm{III}}(y) &\equiv y - y^{21}/21 \\ B_0^{\mathrm{IV}}(y) &\equiv \sinh^{-1}\gamma y - \gamma y(\gamma^2 + 1)^{-1/2}. \end{aligned} \qquad [6]$$

Two numerical results have characterized all runs performed, and, though we have been unable to prove either one analytically, we suspect they are generally true: (*i*) as S or M is raised a first unstable eigenvalue always appears ($\omega_i > 0$) at finite values of S and M with $\omega_r = 0$; and (*ii*) a necessary condition that instabilities appear is that the current profile j_0 shall have an *inflection point* between $y = -1$ and $y = +1$. Steep current gradients alone seem insufficient to produce instability. For example, $B_0^{\mathrm{III}}(y)$, which has a large maximum current gradient of 20 near the walls, was found to be stable up to $M = 10^4$, $S = 10^4$ (for $\alpha = 1$), whereas profiles such as B_0^{II}, which did contain inflection points, would characteristically be unstable for S and M no greater than a few tens, with considerably smaller current gradients involved.

Particularly extensive investigations were carried out for the profile $B_0^{\mathrm{II}}(y)$ for various values of α, S, M, and the "stretching parameter" γ. Fig. 1 is a plot of $B_0^{\mathrm{II}}(y)$ and its associated current profile $j_0^{\mathrm{II}}(y) = -DB_0^{\mathrm{II}}$ as a function of y for $\gamma = 10$. This case will be used to illustrate the results in Figs. 2–9.

Fig. 2 shows typical eigenfunctions, stable and unstable, computed from the B_0^{II} of Fig. 1. Fig. 2*A* applies to $S = M = 10$, for the least-damped eigenvalue $\omega_i = -0.1695$. For this case, $\omega_r = 0$, $\alpha = 1.0$, $b = ib_i$ is purely imaginary, and $v = v_r$ is purely real. This last property always applies to the eigenfunction with the greatest ω_i. Fig. 2*B* shows b_i, v_r for an eigenfunction immediately above the instability threshold, with

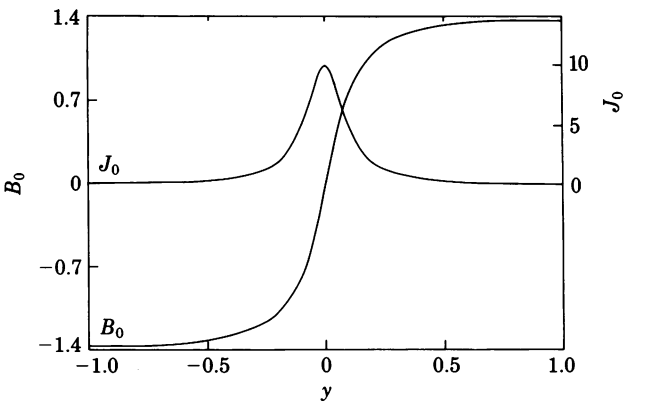

FIG. 1. $B_0 = B_0^{\mathrm{II}}(y)$ and its associated current profile $j_0 = -DB_0$, for $\gamma = 10$.

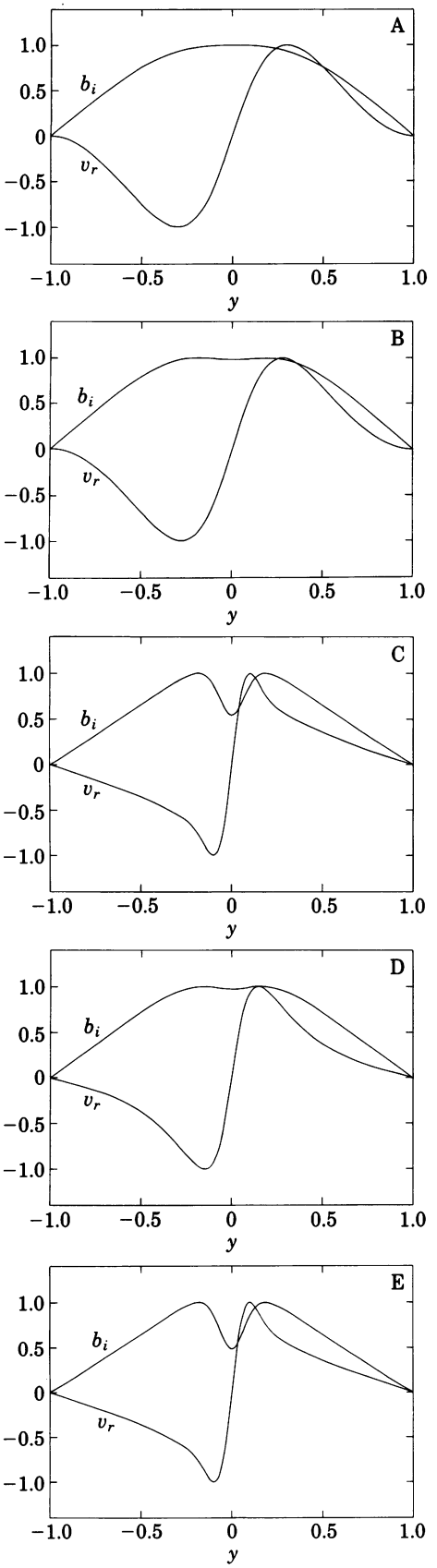

FIG. 2. (*A*) Eigenfunctions $b = ib_i$, $v = v_r$ for the least-damped eigenvalues for $M = 10, S = 10$. (*B*) Eigenfunctions $b = ib_i$, $v = v_r$ slightly above the instability threshold: $M = 20$, $S = 20$. (*C*) Unstable eigenfunctions $b = ib_i$, $v = v_r$ for $S = M = 1{,}000$. (*D*) Unstable eigenfunctions $b = ib_i$, $v = v_r$ for $S = 10$, $M = 10^5$. (*E*) Unstable eigenfunctions $b = ib_i$, $v = v_r$ for $S = 10^5$, $M = 10$.

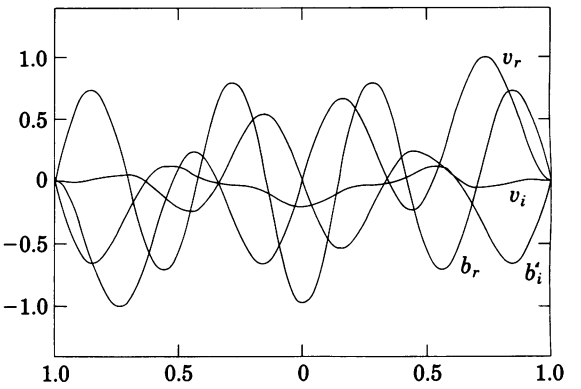

FIG. 3. Highly damped complex eigenfunctions for $M = S = 20$.

$S = M = 20$, $\omega_i = 0.06940$, $\alpha = 1.0$, $\omega_r = 0$. Fig. 2*C* shows b_i, v_r well above the threshold, with $S = M = 1{,}000$, $\alpha = 1.0$, $\omega_i = 0.19687$, and $\omega_r = 0$. Fig. 2*D* shows the case $S = 10$, $M = 10^5$, with $\alpha = 1.0$, $\omega_i = 0.4397$, and $\omega_r = 0$. Fig. 2*E* shows the case $S = 10^5$, $M = 10$, $\omega_i = 0.002537$, $\alpha = 1.0$, $\omega_r = 0$ and illustrates the (perhaps unsurprising) result that viscosity is better at suppressing unstable growth than resistivity.

The damped modes have, in general, both ω_i and ω_r finite. Typical eigenfunctions for a highly damped mode for B_0^{II} are shown in Fig. 3 ($\omega_r = -0.40492$, $\omega_i = -6.01303$, $S = M = 20$, $\alpha = 1.0$).

At the stability threshold $\omega = 0$, the scaling $v' \equiv vM^{-1/2}$, $b' \equiv bS^{-1/2}$ reduces Eqs. 3 and 4 to a pair of equations for v' and b' that depend upon S and M only in the combination $(SM)^{1/2}$ (and, of course, upon α). The neutral stability curve in the SM plane, across which ω_i becomes positive for some α, is therefore a hyperbola, approximately $SM = 231.9$. The computed location of this hyperbola (for B_0^{II} with $\gamma = 10$) is shown in Fig. 4. The relatively low values of the critical Reynolds numbers (two orders of magnitude or more below the corresponding hydrodynamic ones for shear flows) are perhaps the most significant feature of this graph. It is also interesting that for low enough values of either Reynolds number, stability will always result for any fixed value of the other, but because SM increases with temperature, according to kinetic theory estimates (13), at high enough temperatures, we may always expect to be on the unstable side of the boundary.

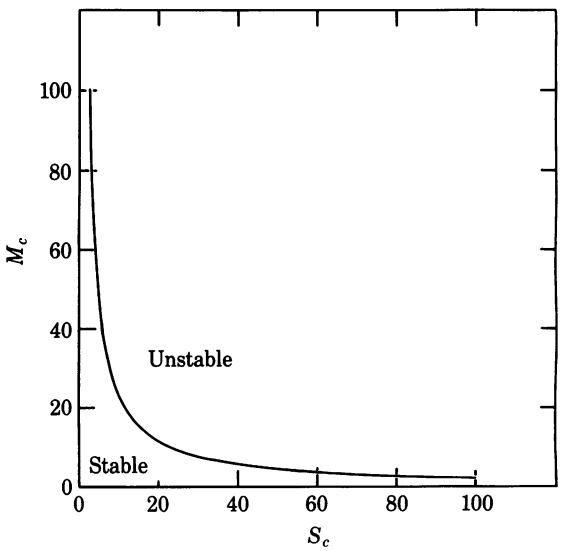

FIG. 4. Locus of critical Reynolds-like numbers $S = S_c$, $M = M_c$ in the MS plane, as determined by computation.

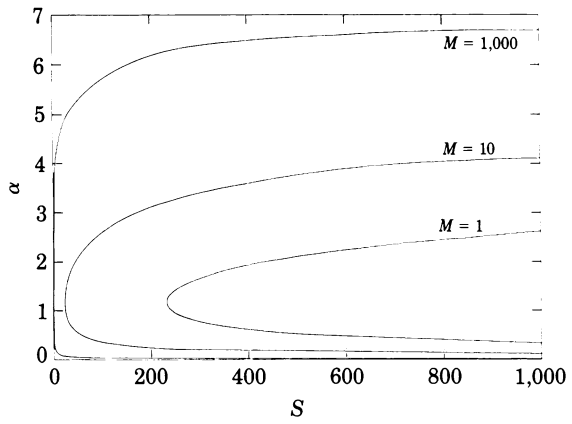

FIG. 5. The neutral stability curve $\omega = 0$ in the α, S plane for M = 1, 10, and 1,000 for B_0^{II} and $\gamma = 10$.

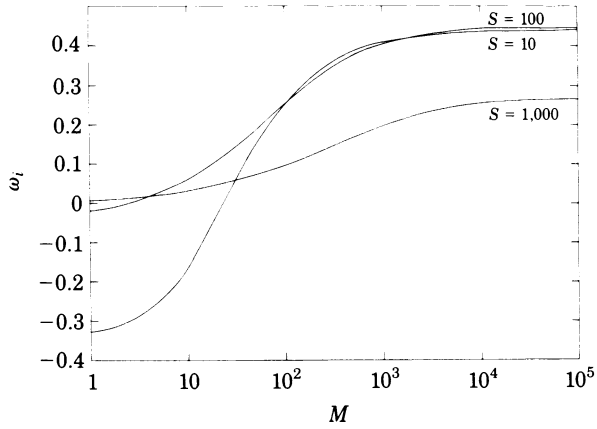

FIG. 7. Growth rate ω_i vs. M for fixed S = 10, 100, and 1,000, α = 1.0, $\gamma = 10$ on B_0^{II}.

To make a comparison with traditional (1) hydrodynamic plots, Fig. 5 exhibits a set of marginal stability curves: $\omega = 0$ in the α, S plane for fixed M for B_0^{II} and $\gamma = 10$. The first unstable α (which, for the reasons previously noted, must be the same for all such curves) is $\alpha = \alpha_c = 1.184 \pm 0.005$. We have generated the *same* curves (not shown) in the α, M plane for fixed S.

Fig. 6*A* shows a growth rate (ω_i vs. S) curve for $M = 10$. Fig. 6*B* shows a logarithmic plot for large values of S, illustrating the $S^{-3/5}$ regime identified analytically by Furth *et al.* (8). Fig. 7 shows the somewhat different behavior of ω_i vs. M for fixed S. Fig. 8 *Upper* shows a contour plot of two periods of the magnetic field lines $\mathbf{B}^{(0)} + \mathbf{B}^{(1)}$ for the B_0^{II} equilibrium plus a 20% admixture of the eigenfunction shown in Fig. 2*B*. Fig. 8 *Lower* shows the streamlines of the velocity field for the same eigenfunction. Fig. 9 shows the growth rate ω_i vs. α for several values of S and M.

The results presented have all been computational and are not the result of an asymptotic "tearing layer" analysis. The marginal stability curves such as Fig. 5 or the stability hyperbola of Fig. 4 could only have been obtained numerically. Despite these results, we are well aware of other potentially im-

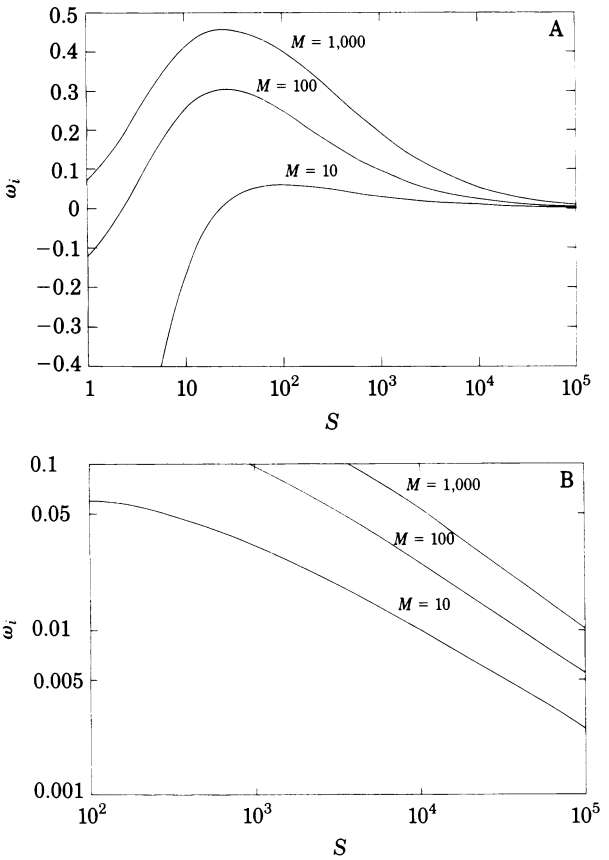

FIG. 6. (*A*) Growth rate ω_i vs. S for $\alpha = 1.0$ (on B_0^{II} with $\gamma = 10$), M = 10, 100, and 1,000. (*B*) Growth rate ω_i vs. S for fixed M, $\alpha = 1.0$, B_0^{II} with $\gamma = 10$.

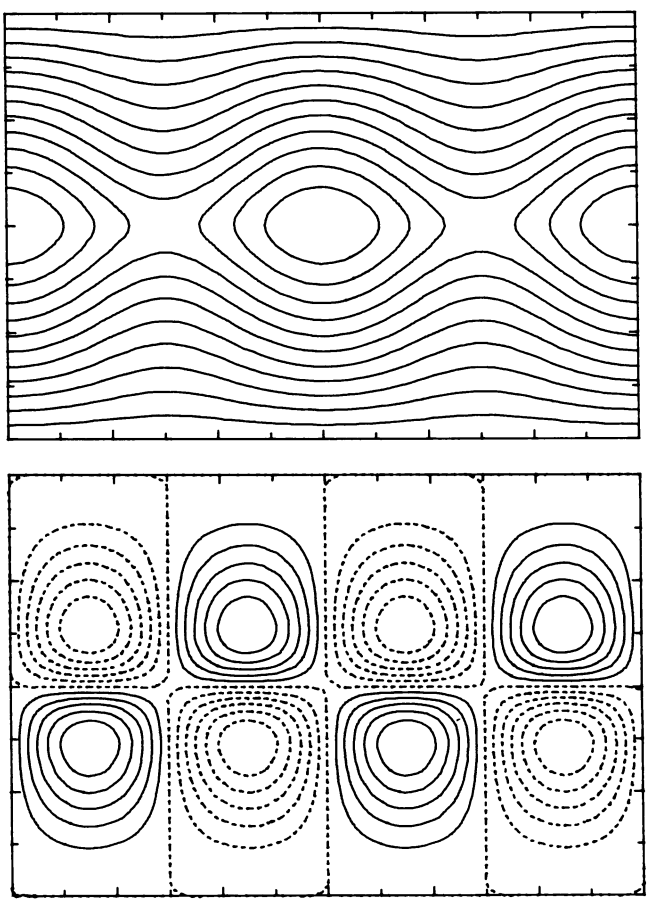

FIG. 8. (*Upper*) Contour plot of magnetic field lines for a typical unstable eigenfunction near the threshold ($S = M = 20$). Field lines are equilibrium plus 20% admixture of eigenfunction. (*Lower*) Velocity streamlines corresponding to eigenfunction represented in *Upper*.

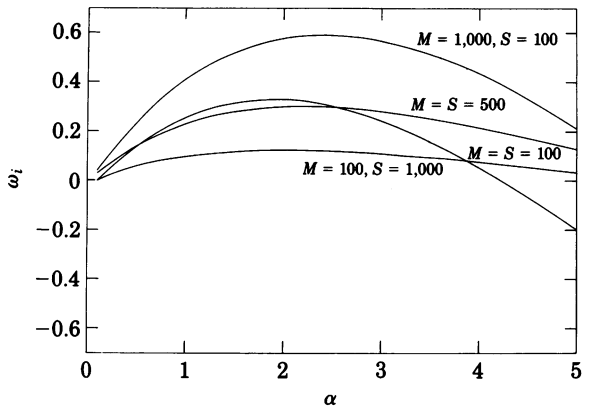

FIG. 9. Growth rate ω_i vs. parallel wavenumber α for B_0^{II}, $M = S = 100$; $M = S = 500$; $M = 1{,}000$, $S = 100$; $M = 100$, $S = 1{,}000$.

portant physical effects that have been left out of the analysis, such as compressibility or the effects of spatially varying viscosity and resistivity tensors. Nevertheless, we believe there to be some value in bringing a more classical hydrodynamic perspective to bear on this highly idealized problem. It is not impossible that subcritical instability thresholds from nonlinear three-dimensional computations may be identified for this problem as they have been for shear flows [see, e.g., Orszag and Kells (19) or Orszag and Patera (20)]. Further computations of a more elaborate kind will be required to test this possibility; for further discussion of the hydrodynamic antecedents, see the review by Herbert (21).

Conversations with Drs. W. H. Matthaeus and G. Vahala are gratefully acknowledged. The work of two of us (R.B.D. and D.M.) was supported in part by National Aeronautics and Space Administration Grant NSG-7416 and by U.S. Department of Energy Contract DE-AS05-76ET53045 at the College of William and Mary. The work of T.A.Z. was supported by National Aeronautics and Space Administration Grant NAG-1-109 at the College of William and Mary. The work of M.Y.H. was supported at the Institute for Computer Applications in Science and Engineering by National Aeronautics and Space Administration Contracts NAS1-16394 and NAS1-15810.

1. Lin, C. C. (1955) *The Theory of Hydrodynamic Stability* (Cambridge Univ. Press, Cambridge, England), pp. 1–75.
2. Maslowe, S. A. (1981) in *Hydrodynamic Instabilities and the Transition to Turbulence*, eds. Swinney, H. L. & Gollub, J. P. (Springer, Berlin), pp. 181–228.
3. Orszag, S. A. (1971) *J. Fluid Mech.* **50**, 689–703.
4. Michael, D. H. (1953) *Proc. Cambridge Philos. Soc.* **49**, 166–168.
5. Stuart, J. T. (1954) *Proc. R. Soc. London Ser. A* **221**, 189–206.
6. Betchov, R. & Criminale, W. O., Jr. (1967) *Stability of Parallel Flows* (Academic, New York), pp. 198–215.
7. Montgomery, D. (1983) in *Spectral Methods in Fluid Mechanics*, eds. Gottlieb, D., Hussaini, M. Y. & Voigt, R. (SIAM, Philadelphia), in press.
8. Furth, H. P., Killeen, J. & Rosenbluth, M. N. (1963) *Phys. Fluids* **6**, 459–484.
9. Furth, H. P., Rutherford, P. H. & Selberg, H. (1973) *Phys. Fluids* **16**, 1054–1063.
10. Wesson, J. (1966) *Nucl. Fusion* **6**, 130–134.
11. Coppi, B., Greene, J. M. & Johnson, J. L. (1966) *Nucl. Fusion* **6**, 101–117.
12. Dibiase, J. A. & Killeen, J. (1977) *J. Comp. Phys.* **24**, 158–185.
13. Braginskii, S. I. (1965) in *Reviews of Plasma Physics*, ed. Leontovich, M. A. (Consultant's Bureau, New York), Vol. 1, pp. 205–309.
14. Reid, W. H. (1965) in *Basic Developments in Fluid Dynamics*, ed. Holt, M. (Academic, New York), pp. 249–307.
15. Lanczos, C. (1956) *Applied Analysis* (Prentice-Hall, New York).
16. Gottlieb, D. & Orszag, S. A. (1977) *Numerical Analysis of Spectral Methods: Theory and Application* (SIAM, Philadelphia).
17. Wilkinson, J. H. (1965) *The Algebraic Eigenvalue Problem* (Oxford Univ. Press, London).
18. Gary, J. & Helgason, R. (1970) *J. Comp. Phys.* **5**, 169–187.
19. Orszag, S. A. & Kells, L. C. (1980) *J. Fluid Mech.* **96**, 159–205.
20. Orszag, S. A. & Patera, T. (1980) *Phys. Rev. Lett.* **45**, 989–993.
21. Herbert, T. (1983) *Stability of Plane Poiseuille Flow—Theory and Experiment* (Virginia Polytechnic Inst. and State Univ., Blacksburg), Rep. VPI-E-81-35.